INTECH
open science | open minds

OPEN ACCESS
ARTICLE

International Journal of Advanced Robotic Systems

Automated Manipulation of Micro-Nano Objects with SPM by Using L_1 Adaptive Controller

Regular Paper

Qinmin Yang[1], Jie Luo[2], Chengyu Cao[2], Jiangang Lu[1,*] and Youxian Sun[1]

1 State Key Laboratory of Industrial Control Technology, Department of Control Science and Engineering, Zhejiang University, China
2 Department of Mechanical Engineering, University of Connecticut, USA
* Corresponding author E-mail: jglu@iipc.zju.edu.cn

Received 6 Jul 2012; Accepted 18 Sep 2012

DOI: 10.5772/53511

Abstract In this paper, a novel control methodology for automatically manipulating micro/nano particles by using a Scanning Probe Microscope (SPM) is presented. First of all, a mathematical model of micro/nanomanipulation, including the interactive forces and dynamics between the tip, particle and substrate along with the roughness effect of the substrate, is described. Then, the L_1 adaptive control design for the manipulation system of micro/nano objects is presented, which consists of a state predictor with fast adaptation, a piece-wise continuous adaptive law and a low-pass filtered control design. This control framework can handle nonlinear uncertainties and ensures uniformly bounded tracking performance. The tracking performance bound can be systematically improved by reducing the step size of integration. Rigorous mathematical proof is provided. Simulation results demonstrate the effectiveness of the presented L_1 adaptive control law on the micro/nanomanipulation model.

Keywords Micro/nanomanipulation, L_1 Adaptive Control, SPM, Nonlinear dynamic systems

1. Introduction

Micro and nano-robotics investigate the handling, manipulation and assembly strategies of objects on both micro and nanoscales. Top-down approaches based on contact manipulation and tweezers have been studied in [1-2] with applications in chemical, material, electronics, pharmaceutical and medical areas. On the other hand, since the invention of the Scanning Probe Microscope (SPM), it has been widely used to provide topographic images with true atomic resolution. Meanwhile, in the recent decades, another advantage of SPM is attributed to the manipulation of micro/nanometre size objects and structures by implementing its probe as a manipulation tool [3]. As a first and critical step for achieving any complex functional micro/nano devices or structures, micro/nanomanipulation techniques can be used for DNA and protein study, data storage and nanotube or surface film characterization, where sub-micron or nanometre scale resolution is imperative.

Traditionally, SPM systems involve 2-D manipulation tasks such as lithography [4], dissection [5] and assembly

[6]. By turning off the servo feedback and applying open-loop control routines, the SPM tip can be lowered towards the substrate and touch the objects, which can be subsequently pushed or pulled mechanically. For the time being, most of the operations have to be done manually [7], which consumes a lot of manpower and time. Therefore, in order to facilitate the transition of nanotechnology products into practical industry, the challenges in fully automatic manipulation and handling of micro/nano objects need to be addressed and overcome.

To this end, an automatic control law to govern the SPM piezoelectric actuators has to be developed. One of the obstacles is that physical and chemical phenomena at the micro/nano scale have not been well understood. Moreover, the forces acting on that scale usually cannot be measured directly. Although extensive studies have been conducted to analyse the adhesive forces between SPM tip, manipulated object and substrate [8-10] in mechanical pushing procedures, an accurate mathematical model with exact expression of the forcesto assist control design for manipulation is still unavailable. Furthermore, some comprehensive beam models have been introduced in the literature [11] by considering the shear deformation and rotary inertia representing the system response in a more highly structured fashion, but they are too difficult for real-time control implementation particularly when augmented with the ever-present nonlinear interaction force [12].

In the meantime, real-time visual information is not available for feedback while the SPM probe is programmed as a manipulation (pushing) tool through the manipulation routine. Hence, a high-level automation scheme is difficult to implement even with the help of augmented virtual reality techniques [7], because only an empirical model is utilized to observe the actual nano environment.

Additionally, SPM tips and usually some of the experimental samples to be manipulated are fragile, which may be easily damaged with improper applied force. Therefore, how to design an appropriate control algorithm for the handling of micro/nano scale objects under the circumstance of high nonlinearities and uncertainties still poses a great challenge.

The control of nonlinear uncertain dynamic systems with unknown disturbance has also attracted extensive interest from the control community [13]. Adaptive control methodologies in particular have been widely adopted to provide systematic solutions for systems whose behaviours can change under different operating conditions [14]. Specifically, in order to cope with the unknown system dynamics within micro/nanomanipulation, an adaptive controller has been recently developed in [15], while neural networks (NN) have also been employed in the controller designs [9]. However, the transient performance of the system cannot be guaranteed due to the learning phase of NN. On the other hand, by constructing a parallel reference system, a novel architecture for the control of nonlinear systems has been developed in [16], named an L_1 adaptive controller. In the presence of unknown high-frequency gain, time-varying unknown parameters and time-varying bounded disturbances, fast adaptation and satisfactory steady responses are delivered.

Therefore, in this paper, an L_1 adaptive feedback controller is discussed to perform autonomous manipulation tasks of micro/nano objects by using an SPM system. It can be proven that the L_1 adaptive controller can ensure a uniformly bounded tracking performance for the SPM piezoelectric drive. The bounds of all the error signals within input and output signals in the sense of L_∞ norm between the actual system and the desired system can be systematically decreased by reducing the time step of integration. Thus, the applied force on the tip and manipulated object can be rendered appropriately. Meanwhile, the nonlinearities within piezo actuators usually arising from high variation in control signal could be mitigated. Finally, the feasibility of the proposed scheme is validated in a simulation environment.

This paper is organized as follows. First, in Section II, the modelling of the micro/nanomanipulation process is presented. Then, the L_1 adaptive control law is developed in Section III. The stability of the overall formation is presented in Section IV and Section V presents numerical simulations. Section VI provides some concluding remarks.

2. Dynamic Model of Manipulation

In this work, only the scenario will be considered that the SPM tip makes contact with a particle and pushes it along the substrate without touching the surface. The drawbacks of manipulation with the tip contacting the surface are discussed in [10] and therefore this is not discussed further in this paper. Also, as a well-recognized problem, thermal drift has been extensively researched in the literature [17-18] and thus is assumed to be compensated for along the manipulation process.

Furthermore, various motion modes, including sliding, rolling and spinning ,have been investigated in [10], and only the sliding mode is reported to most likely happen in a pushing manipulation task. Next, interactive forces are presented and a dynamic model to assist controller design is introduced.

2.1 Interaction Forces

Firstly, the interaction forces between the SPM tip, particle and substrate after the tip contacts the particle are shown in Figure 1 [10].

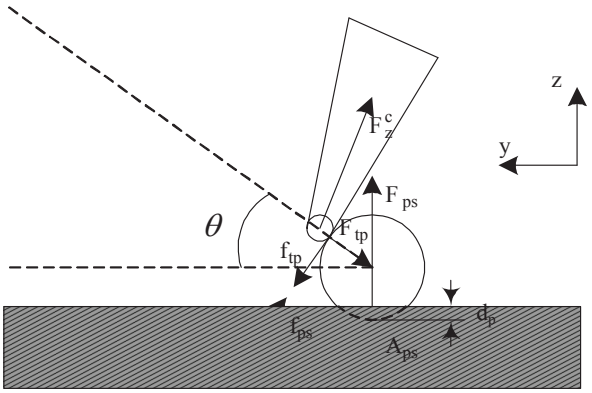

Figure 1. The interacting forces between the SPM tip, particle and substrate.

In this work, the SPM tip apex is assumed to be a spherical ball with radius R_t and the particle radius is denoted as R_p. θ is the pushing angle, which is defined as the angle between the pushing direction and the horizontal plane. A_{ps} is the adhesion force between the particle and substrate. F_{ps} and F_{tp} denote the particle-substrate and the tip-particle attractive/repulsive interaction force, while f_{ps} and f_{tp} correspond to the frictional forces for the particle-substrate and tip-particle, respectively. Elastic deformation of the particle is possible and here only the elastic deformation between the particle and the substrate is considered. The indentation is denoted as d_p.

Moreover, gravitational forces are relatively very small at the nano scale and, thus, are neglected [8]. The main components of the adhesion forces are van der Waals, capillary and electrostatic forces [8-9]. Therefore, the adhesion force between particle and substrate can be given by $A_{ps} = A_{ps}^{vdw} + A_{ps}^{cap} + A_{ps}^{es}$.

i) van der Waals force: $A_{ps}^{vdw} = \dfrac{2HR_p^3}{3h^2(h+2R_p)^2}\left(\dfrac{h}{h+b/2}\right)^2$

ii) Capillary force: $A_{ps}^{cap} = 4\pi\gamma R_p\left(1-\dfrac{h-2e}{2r}\right)$

iii) Electrostatic force: neglected for conducting particle.

where H is the Hamaker constant, h is the particle-substrate distance and b is the peak to peak height of the surface irregularity. γ is the liquid (water) surface energy, e is the thickness of the water layer and r is the adius of curvature of the meniscus formed within the water layer. More details of the analysis of these contact and friction forces can be found in [2, 9], and the reference therein. It has to be noted that, in our controller design to be discussed in the next section, the exact values of those forces are not required to be known.

2.2 Dynamic Model

A satisfactory dynamic model of the pushing mechanism on a planar substrate is formulated in [8] and [9] considering all of the forces mentioned above. Usually, the microscope stage instead of the tip is driven by piezoelectric actuators to achieve a proper pushing force for the micro/nano particle. Therefore, a simplified differential equation governing the system can be given as [8]

$$\begin{aligned}
&\frac{1}{w_x^2}\ddot{x}_s + \frac{1}{w_x Q_x}\dot{x}_s + x_s + \cos\theta f_{ps} = u_x \\
&\frac{1}{w_y^2}\ddot{y}_s + \frac{1}{w_y Q_y}\dot{y}_s + y_s + \sin\theta f_{ps} = u_y \\
&\frac{1}{w_z^2}\ddot{z}_s + \frac{1}{w_z Q_z}\dot{z}_s + z_s + F_{ps} = u_z + A_{ps}
\end{aligned} \tag{1}$$

where (x_s, y_s, z_s) is the position of the stage on x, y, and z axis, respectively. (w_x, w_y, w_z) is the resonant frequency and (Q_x, Q_y, Q_z) is the amplification factor for the stage, which can be measured or obtained from producer. (u_x, u_y, u_z) is the stage driving force generated by the internal piezoelectric actuators which can be seen as the control input signal. Now f_{ps} is the friction force and F_{ps} is the attractive/repulsive interaction force between the particle and substrate, which are apparently nonlinear and uncertain functions of the pushing environment. For more details, please refer to [8] and [9].

For simplification purposes, equation (1) representing the manipulation system can be viewed as a second order nonlinear dynamic system and rewritten as follows

$$\ddot{x} = f(x, \dot{x}) + Wu + d(t) \tag{2}$$

where $x \equiv \begin{bmatrix} x_s & y_s & z_s \end{bmatrix}^T$ is the system state and $u \equiv \begin{bmatrix} u_x & u_y & u_z \end{bmatrix}^T$ is the control input. Since the interaction forces between particle, substrate and tip cannot be exactly known, the function $f(\cdot): \mathbb{R}^6 \to \mathbb{R}^3$ is considered to be an uncertain nonlinear smooth function matrix. $d(t) \in \mathbb{R}^3$ represents the unknown external disturbance and the constant diagonal matrix $W \in \mathbb{R}^{3\times 3}$ is defined as

$$W \equiv \begin{bmatrix} w_x^2 & 0 & 0 \\ 0 & w_y^2 & 0 \\ 0 & 0 & w_z^2 \end{bmatrix} \tag{3}$$

whose eigenvalues are always positive. Thereafter, the objective of the controller design is to drive the stage to follow a desired trajectory $x_d = \begin{bmatrix} x_{sd} & y_{sd} & z_{sd} \end{bmatrix}^T$ and guarantee a desired applied force on the cantilever at the same time. Since the lateral force has a direct effect on the

deflection of the probe along the *z*axis ζ_z, which is observed to be a function of the pushing angle θ [9], the control goal can be translated to keeping a desired trajectory z_d during the pushing procedure by assuming that the topographic information of the substrate surface has been obtained beforehand.

Note 1: In [8-9], ζ_z is employed as a control objective to be kept constant along the pushing task. However, the desired value of ζ_z is usually hard to achieve *a priori*, since it is dependent on the pushing speed, the experimental setting and other unknown factors. As a matter of fact, typically, freshly cleaved mica is utilized as the substrate for manipulation experiments because of its relatively smooth and hard surface [17]. The root mean square (RMS) roughness of the mica surface isin the order of0.01 nm [19]. Hence, it is believed to be more convenient and efficient to maintain a desired z_d.

Next, the following assumptions are proposed before going forward.

Assumption 1: The disturbance $d(t)$ is bounded above such that $\|d(t)\| \le d_m$, where $d_m \in \mathbb{R}^+$ is an unknown positive constant with $\|\cdot\|$ standing for the standard Euclidean norm.

Assumption 2: The unknown nonlinear function $f(\cdot)$ satisfies the semiglobal Lipschitz condition, i.e., for any $\delta > 0$, there exist $L(\delta) > 0$ and $B > 0$ such that $\|f(X_1) - f(X_2)\|_\infty \le L(\delta)\|X_1 - X_2\|_\infty$, and $\|f(0)\| \le B$, for all $\|X_i\|_\infty \le \delta$, $i = 1,2$ uniformly.

Note 2: Assumption 1 and 2 are commonly found in the control literature [14]. Furthermore, it can be readily verified as reasonable for the real SPM system to undertake the micro/nanomanipulation process through the analysis in section 2.1.

3. L_1 Adaptive Controller Design

In this section, how to design the L_1 adaptive controller for the micro/nano manipulation via the tip of the SPM is introduced. Firstly, the original system (2) can be rephrased in lower triangular form as

$$\begin{aligned} \dot{x}_1 &= x_2 \\ \dot{x}_2 &= f(x_1, x_2) + Wu + d(t) \end{aligned} \tag{4}$$

with $x_1 = x$, $x_2 = \dot{x}$ and initial condition $x_1(0) = x_0$.

Thereafter, the following state predictor is developed as

$$\begin{aligned} \dot{\hat{x}}_1 &= \hat{x}_2 + \hat{\sigma}_1 \\ \dot{\hat{x}}_2 &= A_{m1}\hat{x}_1 + A_{m2}\hat{x}_2 + Wu + \hat{\sigma}_2 \end{aligned} \tag{5}$$

with $\hat{x}_1(0) = x(0)$, $\hat{x}_2(0) = \dot{x}(0)$. A_{m1}, $A_{m2} \in \mathbb{R}^{3\times 3}$ are user defined, such that $A_m = \begin{bmatrix} 0 & I_3 \\ A_{m1} & A_{m2} \end{bmatrix}$ is Hurwitz. A straightforward choice of A_m is $\begin{bmatrix} 0 & I_3 \\ a_{m1}I_3 & a_{m2}I_3 \end{bmatrix}$, where a_{m1}, $a_{m2} \in \mathbb{R}^-$ are negative constants and $I_3 \in \mathbb{R}^{3\times 3}$ is the identity matrix. $\hat{X} \equiv \begin{bmatrix} \hat{x}_1^T & \hat{x}_2^T \end{bmatrix}^T$ is the estimate of system state vector $X \equiv \begin{bmatrix} x_1^T & x_2^T \end{bmatrix}^T$, where $\hat{x}_1 \equiv \begin{bmatrix} \hat{x}_s & \hat{y}_s & \hat{z}_s \end{bmatrix}^T$, and the prediction error is defined as $\tilde{X} = \hat{X} - X = \begin{bmatrix} \tilde{x}_1^T & \tilde{x}_2^T \end{bmatrix}^T$. $\hat{\sigma}_1 \in \mathbb{R}^3$ and $\hat{\sigma}_2 \in \mathbb{R}^3$ are the adaptive estimate of the remaining dynamics.

Thereafter, the adaptation laws are designed to be

$$\begin{aligned} \begin{bmatrix} \hat{\sigma}_1(t) \\ \hat{\sigma}_2(t) \end{bmatrix} &= \begin{bmatrix} \hat{\sigma}_1(iT_s) \\ \hat{\sigma}_2(iT_s) \end{bmatrix}, \quad t \in [iT_s, (i+1)T_s) \\ \begin{bmatrix} \hat{\sigma}_1(iT_s) \\ \hat{\sigma}_2(iT_s) \end{bmatrix} &= -\Phi^{-1}(T_s)\mu(iT_s) \end{aligned} \tag{6}$$

where

$$\begin{aligned} \Phi(T_s) &= A_m^{-1}(e^{A_m T_s} - I_6) \\ \mu(iT_s) &= e^{A_m T_s}\tilde{X}(iT_s), \qquad i = 0,1,2,... \end{aligned} \tag{7}$$

$I_6 \in \mathbb{R}^{6\times 6}$ is the identity matrix and $T_s > 0$ is the adaptation sampling time, which is determined by the clock speed of the DSP chip within the microscope controller.

Then, the control law is proposed as follows

$$\begin{aligned} u(s) = &-C_2(s)W^{-1}\hat{\sigma}_2(s) - C_1(s)H_m(s)^{-1}H_{um}(s)W\hat{\sigma}_1(s) \\ &+k_g x_r(s) \end{aligned} \tag{8}$$

where $k_g = -a_{m1}^3 W^{-1}$, $H_m(s) = W/(s^2 - a_{m2}s - a_{m1})$ and $H_{um}(s) = (s - a_{m2})W^{-1}/(s^2 - a_{m2}s - a_{m1})$. Here $C_1(s)$ and $C_2(s)$ are low-pass filters with a unit DC gain as

$$\begin{aligned} C_1(s) &= k_1/(s + k_1) \\ C_2(s) &= k_2/(s + k_2) \end{aligned} \tag{9}$$

$C_1(s)$ needs to ensure that $C_1(s)H_m(s)^{-1}H_{um}(s)$ is strictly-proper. $\hat{\sigma}_i(s)$, $i = 1,2$ is the Laplace transformations of $\hat{\sigma}_i(t)$ .Furthermore, x_r is a bounded reference input signal which can generate the desired output x_d for the following nominal system.

$$\begin{aligned} \dot{x}_{n1} &= x_{n2} \\ \dot{x}_{n2} &= A_{m1}x_{n1} + A_{m2}x_{n2} + Wk_g x_r \end{aligned} \tag{10}$$

In order to assist the proof of the stability of the closed-loop system, the following preliminary terms are defined. Let

$$\begin{aligned}\tau_1(s) &= \begin{bmatrix} C_1(s)H_m(s)^{-1}H_{um}(s)W & C_2(s)W^{-1} \end{bmatrix} \\ &= \begin{bmatrix} C_2(s) & C_1(s)H_m(s)^{-1}H_{um}(s) \end{bmatrix} \begin{bmatrix} 0 & W^{-1} \\ W & 0 \end{bmatrix}\end{aligned} \tag{11}$$

and the norm of $\tau_2(s)$ is given by

$$\|\tau_2\| = \left\| (sI - A_m)^{-1} \begin{bmatrix} 0 \\ W \end{bmatrix} \right\|_{L_1} \|\tau_1\|_{L_1} + \left\| (sI - A_m)^{-1} \right\|_{L_1} \tag{12}$$

Further, let

$$\eta_1(T_s) = \int_0^{T_s} \left\| e^{A_m(T_s - \tau)} \right\| d\tau \tag{13}$$

and

$$\nu(T_s) = \eta_1(T_s)\left(L(\gamma_x)\gamma_x + B + d_m \right) \tag{14}$$

where γ_x is introduced later. Define

$$\beta_1(T_s) = \max_{t \in [0, T_s]} \int_0^t \left\| e^{A_m(t-\tau)} \right\| d\tau \tag{15}$$

$$\beta_2(T_s) = \max_{t \in [0, T_s]} \int_0^t \left\| e^{A_m t} \right\| d\tau \tag{16}$$

and

$$\begin{aligned}\gamma_{\tilde{x}} = {} & \beta_2(T_s)\nu(T_s) + 2\beta_1(T_s)\left(L(\gamma_x)\gamma_x + B + d_m \right) \\ & + \beta_1(T_s)\sqrt{\lambda_{\max}(A_m^T A_m)}\nu(T_s)\end{aligned} \tag{17}$$

where $\lambda_{\max}(\cdot)$ denotes the maximum eigenvalue.

Moreover, the choices of $C(s)$ and sampling time T_s need to ensure γ_x exists such that

$$\begin{aligned}\gamma_x > {} & \|\tau_2\| \sqrt{\lambda_{\max}(A_m^T A_m)}\nu(T_s) + \|x_d\|_{L_\infty} \\ & + \|\tau_2\| \left(L(\gamma_x)\gamma_x + B + d_m \right) + \gamma_{\tilde{x}}\end{aligned} \tag{18}$$

Next, the performance bounds of the L_1 adaptive control system are theoretically proven.

First, the error dynamics is obtained by subtracting (4) from (5) as

$$\begin{aligned}\dot{\tilde{x}}_1 &= \tilde{x}_2 + \hat{\sigma}_1 \\ \dot{\tilde{x}}_2 &= A_{m1}\hat{x}_1 + A_{m2}\hat{x}_2 + \hat{\sigma}_2 - f - d\end{aligned} \tag{19}$$

Hence, the theoretical results on the performance bounds of the closed-loop system (4) with the L_1 controller can be presented.

Theorem 1: Let the sampling time T_s be chosen to be sufficiently small. Given the closed–loop system (2) with the L_1 controller defined via (6)–(9) subject to the L_1–norm conditions in (9) and (18), if $\|X(0)\|_\infty \le \gamma_x$, then the bounds of all signals within the closed-loop system satisfy

$$\|\tilde{X}\|_{L_\infty} \le \gamma_{\tilde{x}} \tag{20}$$

$$\|X\|_{L_\infty} \le \gamma_x \tag{21}$$

and

$$\|u\|_{L_\infty} \le \gamma_u \tag{22}$$

where $\gamma_{\tilde{x}}$ and γ_x is introduced in (17) and (18) respectively, and

$$\begin{aligned}\gamma_u = {} & \|\tau_1\| \sqrt{\lambda_{\max}(A_m^T A_m)}\nu(T_s) + \|\tau_1\| \left(L(\gamma_x)\gamma_x + B + d_m \right) \\ & + \|k_g x_r\|_{L_\infty}\end{aligned} \tag{23}$$

Proof: First of all, since the initial condition satisfies $\|X(0)\|_\infty \le \gamma_x$ and $X(t)$ is continuous, we assume that time t' exists such that

$$\|X(t')\|_\infty = \gamma_x, \text{ while } \|X(t)\|_\infty < \gamma_x, \forall t \in [0, t') \tag{24}$$

which implies that

$$\|X_{t'}\|_{L_\infty} = \gamma_x \tag{25}$$

where $\|X_{t'}\|_{L_\infty}$ denotes the truncated L_∞ norm of X at the time instant t'.

It immediately follows (19) that

$$\begin{aligned}\tilde{X}(iT_s + t) = {} & e^{A_m T_s}\tilde{X}(iT_s) + \int_0^t e^{A_m(t-\tau)}\hat{\sigma}(iT_s)d\tau \\ & - \int_0^t e^{A_m(t-\tau)}\Lambda\left(f(iT_s + \tau) + d(iT_s + \tau) \right)d\tau\end{aligned} \tag{26}$$

where

$$\Lambda = \begin{bmatrix} 0 \\ I_3 \end{bmatrix} \tag{27}$$

for the simplification purpose. Equation (26) further implies

$$\begin{aligned}\tilde{X}((i+1)T_s) = {} & e^{A_m T_s}\tilde{X}(iT_s) + \int_0^{T_s} e^{A_m(T_s - \tau)}\hat{\sigma}(iT_s)d\tau \\ & - \int_0^{T_s} e^{A_m(T_s - \tau)}\Lambda\left(f(iT_s + \tau) + d(iT_s + \tau) \right)d\tau\end{aligned} \tag{28}$$

Substituting (6) into (28) yields

$$\tilde{X}((i+1)T_s) = -\int_0^{T_s} e^{A_m(T_s - \tau)}\Lambda\left(f(iT_s + \tau) + d(iT_s + \tau) \right)d\tau \tag{29}$$

Since the system satisfies the Lipschitz condition, i.e., $\|f(X)\| \le L(\gamma_x)\gamma_x + B$, and $\|d(t)\| \le d_m$ for $t \in [0, t']$, utilizing (13) and (14) results in

$$\|\tilde{X}((i+1)T_s)\| \le \eta_1(T_s)\left(L(\gamma_x)\gamma_x + B + d_m\right) = \nu(T_s) \quad (30)$$

for $(i+1)T_s \in [0, t']$.

According to the choice of adaptive law (6), one has

$$e^{A_m T_s}\tilde{X}(iT_s) + \int_0^{T_s} e^{A_m(T_s-\tau)}\hat{\sigma}(iT_s)d\tau = 0 \quad (31)$$

which further shows

$$\begin{aligned}\tilde{X}(iT_s) &= (I - e^{A_m T_s})\tilde{X}(iT_s) - \int_0^{T_s} e^{A_m(T_s-\tau)}\hat{\sigma}(iT_s)d\tau \\ &= -\int_0^{T_s} e^{A_m(T_s-\tau)}(\hat{\sigma}(iT_s) + A_m\tilde{X}(iT_s))d\tau\end{aligned} \quad (32)$$

Meanwhile, (29) provides

$$\tilde{X}(iT_s) = -\int_0^{T_s} e^{A_m(T_s-\tau)}\Lambda\left(f((i-1)T_s+\tau) + d((i-1)T_s+\tau)\right)d\tau \quad (33)$$

Hence, (32) and (33) together imply

$$\begin{aligned}&\int_0^{T_s} e^{A_m(T_s-\tau)}\Lambda\left(f((i-1)T_s+\tau) + d((i-1)T_s+\tau)\right)d\tau \\ &= \int_0^{T_s} e^{A_m(T_s-\tau)}(\hat{\sigma}(iT_s) + A_m\tilde{X}(iT_s))d\tau\end{aligned} \quad (34)$$

Following (30) and (34), one obtains the following upper bound by consulting standard linear algebra

$$\|\hat{\sigma}(iT_s)\| \le \sqrt{\lambda_{\max}(A_m^T A_m)}\nu(T_s) + L(\gamma_x)\gamma_x + B + d_m \quad (35)$$

for $iT_s \in [0, t']$.

Subsequently, for all $iT_s + t \le t'$, where $0 \le t \le T_s$, by referring to (26) and (30), and the definition of $\beta_1(T)$, $\beta_2(T)$ in (15) and (16), one reaches the following upper bound as

$$\begin{aligned}\|\tilde{X}(iT_s + t)\| \le{}& \beta_2(T_s)\nu(T_s) + \beta_1(T_s)\sqrt{\lambda_{\max}(A_m^T A_m)}\nu(T_s) \\ &+2\beta_1(T_s)\left(L(\gamma_x)\gamma_x + B + d_m\right)\end{aligned} \quad (36)$$

which directly gives that

$$\|\tilde{X}(t)\| \le \gamma_{\tilde{x}} \quad (37)$$

for all $t \in [0, t']$ from (17).

Furthermore, since $\tilde{X} = \hat{X} - X$, and naturally

$$\|X(t)\| \le \|\tilde{X}(t)\| + \|\hat{X}(t)\| \quad (38)$$

it follows from (5) that

$$\begin{aligned}\hat{X}(t) = (sI - A_m)^{-1}\begin{bmatrix}0\\W\end{bmatrix}u(s) + (sI - A_m)^{-1}\hat{\sigma}(s) \\ +(sI - A_m)^{-1}x(0)\end{aligned} \quad (39)$$

Thus, one has the following upper bound as

$$\begin{aligned}\|\hat{X}_{t'}\|_{L_\infty} \le{}& \left\|(sI - A_m)^{-1}\begin{bmatrix}0\\W\end{bmatrix}\right\|_{L_1}\|u_{t'}\|_{L_\infty} + \left\|(sI - A_m)^{-1}\right\|_{L_1}\|\hat{\sigma}_{t'}\|_{L_\infty} \\ &+\|x_0\|_{L_\infty}\end{aligned} \quad (40)$$

over $t \in [0, t']$, where $x_0(s) = (sI - A_m)^{-1}x_0$.

Meanwhile, recalling (8) results in the upper bound of control signal

$$\|u_{t'}\|_{L_\infty} \le \|\tau_1\|_{L_1}\|\hat{\sigma}_{t'}\|_{L_\infty} + \|k_g x_{r_{t'}}\|_{L_\infty} \quad (41)$$

where τ_1 is defined in (11). Substituting (41) into (40) yields

$$\|\hat{X}_{t'}\|_{L_\infty} \le \|\tau_2\|\|\hat{\sigma}_{t'}\|_{L_\infty} + \|\bar{x}_{r_{t'}}\|_{L_\infty} \quad (42)$$

where τ_2 is defined in (12), and

$$\|\bar{x}_{r_{t'}}\|_{L_\infty} = \left\|(sI - A_m)^{-1}\begin{bmatrix}0\\W\end{bmatrix}\right\|_{L_1}\|k_g x_{r_{t'}}\|_{L_\infty} + \|x_0\|_{L_\infty}.$$

Therefore, by resorting to (35), one has

$$\begin{aligned}\|\hat{X}_{t'}\|_{L_\infty} \le{}& \|\tau_2\|\sqrt{\lambda_{\max}(A_m^T A_m)}\nu(T_s) + \|\tau_2\|(L(\gamma_x)\gamma_x + B + d_m) \\ &+\|\bar{x}_{r_{t'}}\|_{L_\infty}\end{aligned} \quad (43)$$

Eventually, by combining (37), (38) and (43), one gets the upper bound of $X(t)$ as

$$\begin{aligned}\|X_{t'}\|_{L_\infty} \le{}& \|\tau_2\|\sqrt{\lambda_{\max}(A_m^T A_m)}\nu(T_s) + \|\bar{x}_{r_{t'}}\|_{L_\infty} \\ &+\|\tau_2\|(L(\gamma_x)\gamma_x + B + d_m) + \gamma_{\tilde{x}}\end{aligned} \quad (44)$$

Considering the stability condition, (44) becomes

$$\|X_{t'}\|_{L_\infty} < \gamma_x \quad (45)$$

which contradicts (25). Thus, it shows (21) is true and (20) is a direct outcome of (21) and (37). Furthermore, by consulting (21), (35) and (41), one has

$$\begin{aligned}\|u\|_{L_\infty} <{}& \|\tau_1\|\sqrt{\lambda_{\max}(A_m^T A_m)}\nu(T_s) + \|\tau_1\|(L(\gamma_x)\gamma_x + B + d_m) + \|k_g x_r\|_{L_\infty} \\ &< \gamma_u\end{aligned} \quad (46)$$

which proves (22) and concludes the proof of Theorem 1.

Note3: By making the bandwidth of the low-pass filters $C_1(s)$ and $C_2(s)$ large enough, the control law (8) can ensure that $\lim_{s\to 0} \hat{x}_1(s) = x_d(s)$. Therefore, Theorem 1 together with the control law can guarantee that the difference between $x(t)$ and $x_d(t)$ is bounded. Moreover, the bound can be reduced arbitrarily by decreasing the integration time step T_s.

4. Simulation Results

In this section, the proposed controller is applied toa manipulation task via the SPM system in a simulation environment. The control objective is to guide the stage movement to follow a desired trajectory such that an appropriate push force can be applied on the cantilever and also the particle.

The dynamics of the stage is modelled as (1) with $w_{x,y,z} = 2\pi f_{x,y,z}$, $f_{x,y} = 250Hz$, $f_z = 18.7Hz$ and $Q_{x,y,z} = 20$ in the simulation [20]. The manipulation task is assumed to be pushing a nano scale particle along a direct line over a mica surface with a constant prescribed speed $v = 1000nm/s$. The angle between y axis and the pushing direction is set to be $30°$, i.e., $x_{sd}(t) = 1000\sin(30°)t$ and $y_{sd}(t) = 1000\cos(30°)t$. Meanwhile, $R_p = 30nm$ in the simulation. To imitate reality and test the robustness of the control method under the roughness effects, the substrate surface is set as a sinusoid function with the amplitude of 0.1 nm. A bounded uniformly distributed external environmental noise d is imposed with a bound of $d_m = 1\ nN$.

The controller parameters used in this simulation are tabulated as below.

Parameter	a_{m1}	a_{m2}	k_1, k_2	T_s
Value	-20	-40	50	1×10^{-3}

Table 1. Summary of parameters used in the simulation

It has to be noted that the low-pass filters $C_1(s)$ and $C_2(s)$ are rendered the same to simplify the controller structure.

A typical system response using the proposed controller is shown in Figure 2 including the stage trajectory on x, y and z directions. Simulation results demonstrate that the L1adaptive controller can drive the SPM stage to follow a preset curve with the presence of unknown system dynamics and external disturbance. The control input trajectories are also depicted in Figure 3, which verifies the boundedness of the control signals (u_x, u_y, u_z). Moreover, the deflection of the probe along the z axis ζ_z is also plotted in Figure4. It shows that during the initial phase when the probe makes contact with the nano object, there is a sharp spike on the deflection. But as the stage is driven by the actuators, the nano particle is moved by the probe and the deflection converges to a constant value – approximately 0.2 nm.

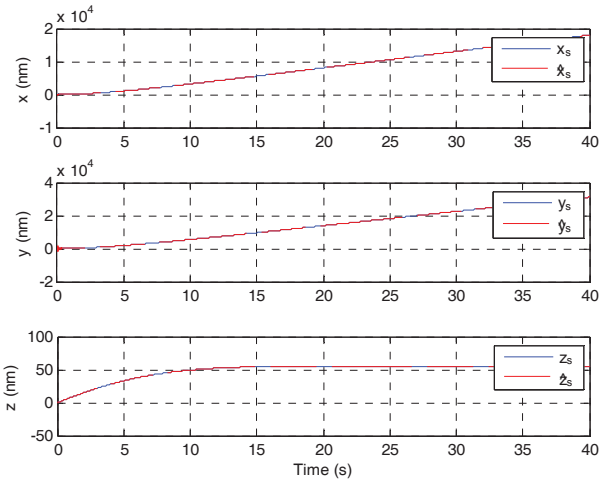

Figure 2. Simulation results of the proposed controller on the micro/nanomanipulation system: trajectories of the actual movement of the stage (solid lines) and the output of the state predictor (dashed lines).

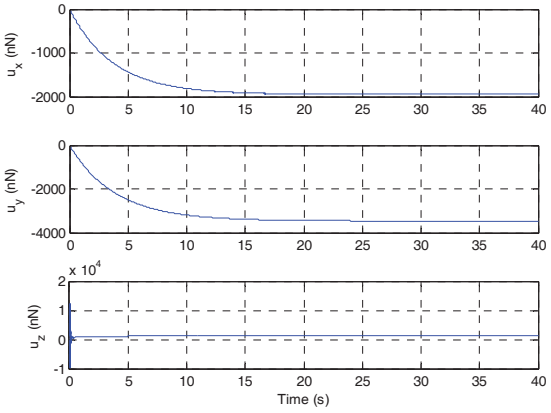

Figure 3. Simulation results of the proposed controller on the micro/nanomanipulation system: control input.

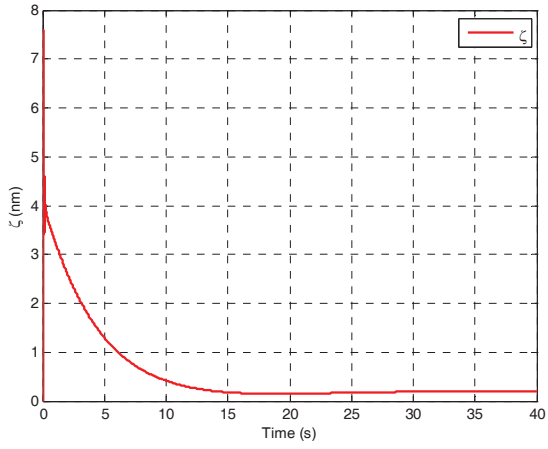

Figure 4. Simulation results of the proposed controller on the micro/nanomanipulation system: trajectory of ζ_z.

In order to evaluate the sensitivity of the controller to parameter variations and test its robustness, a different set of parameters is adopted in the simulation as in Table 2.

Parameter	a_{m1}	a_{m2}	k_1, k_2	T_s
Value	-10	-20	20	1×10^{-3}

Table 2. Summary of parameters used in the second simulation

The system response including the stage trajectory and control input on x, y and z directions is shown in Figure5 and 6, respectively. Furthermore, the deflection of the probe along the z axis ζ_z is also plotted in Figure7. The simulation results show the uniformly bounded tracking performance of the system even with different control parameters, although the convergence rate of the system is a bit smaller.

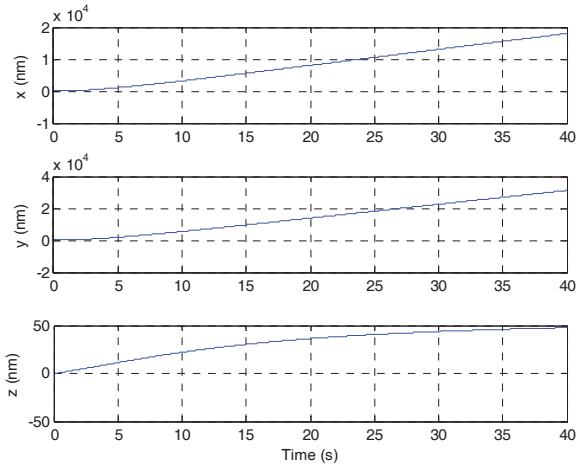

Figure 5. Simulation results of the proposed controller with a different set of parameters on the micro/nanomanipulation system: trajectories of the actual movement of the stage.

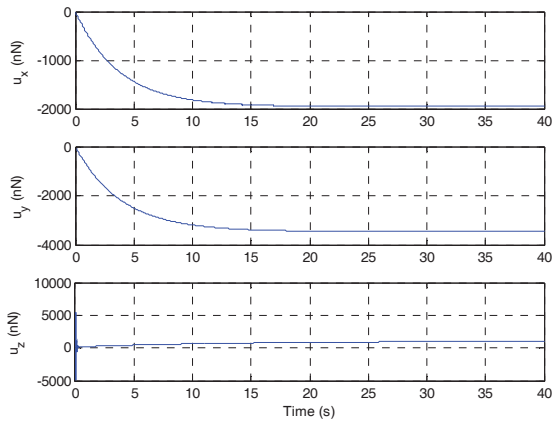

Figure 6. Simulation results of the proposed controller with a different set of parameterson themicro/nanomanipulation system: control input.

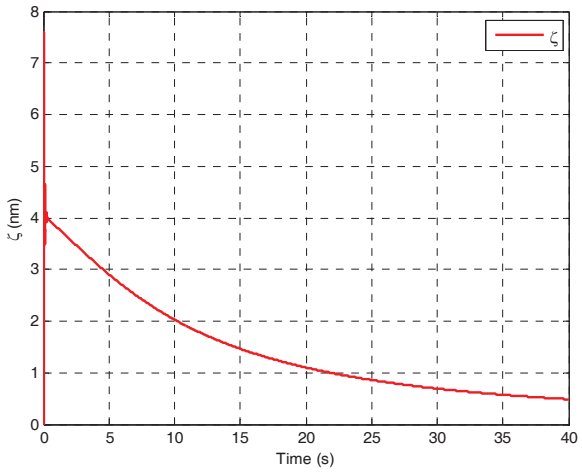

Figure 7. Simulation results of the proposed controller with a different set of parameterson the micro/nanomanipulation system: trajectory of ζ_z .

5. Conclusion

The task of manipulating micro/nano particles by SPM is complex and time-consuming to operate manually. In order to automate this, anL1 adaptive controller is designed for guiding the stage so that the position of the micro/nano particle follows a predefined trajectory with proper applied force imposed on it. The controller consists of a state predictor, a piece-wise continuous adaptive law and a low-pass filtered control law. This control framework ensures uniformly bounded tracking for the system. The performance bound can be systematically improved by reducing the step size of integration. The low-pass filtered control signal is also ensured to relax the requirement of actuator bandwidth and thus mitigate the incurred nonlinearities of the piezoelectric actuators. Furthermore, the stability of the control system is verified theoretically. Finally, the feasibility of our method is demonstrated through the simulation results. In future work, we will consider implementing the presented controller in the practical SPM system for manipulation tasks.

6. Acknowledgments

We would like to thank the associate editor and the reviewers for their time in handling this article. This work is supported by National Natural Science Foundation (NNSF) of China under grant no. 61104008, Qianjiang Programme of Zhejiang Province under grant no. 2011R10024, Commonweal Technology Research Foundation of Zhejiang Province under grant no. 2011C31021,and Research Fund for the Doctoral Programme of Higher Education of China under grant no. 20110101120063.

7. References

[1] K. Rabenorosoa, C. Clevy, Q. Chen and P. Lutz, "Study of forcesduring micro-assembly tasks using two-sensing-fingers gripper,"IEEE/ASME Transactions on Mechatronics, vol. 17, no. 5, pp. 811–821, 2012

[2] M. Gauthier and S. Regnier, Robotic Micro-assembly, IEEE Press,Wiley Edition, 2010.

[3] A. A. G. Requicha, "Nanomanipulation with the atomic force microscope," in R. Waser, Ed. Nanotechnology, Volume 3: Information Technology. Weinheim, Germany: Wiley-VCH, pp. 239-273, 2008.

[4] Z. Liu, Z. Li, G. Wei, Y. Song, L. Wang and L. Sun, "Manipulation, dissection and lithography using modified tapping mode atomic force microscope," Microsc. Res. Tech., vol. 69, no. 12, pp. 998–1004, 2006.

[5] J. H. Lv, "Nanomanipulation of extended single-DNA molecules on modified mica surfaces using the atomic force microscopy,"Colloids and Surfaces B: Biointerfaces, vol. 39, no. 4, pp. 177–180, 2004.

[6] K. Xu, C. Wu, X. Tian, Y. Zhang, Z. Dong, "A Method Study on Assembly of Single-Wall Carbon Nanotube Field Effect Transistor Using Dielectrophoresis," Advanced Materials Research, vols.139-141, pp. 1550-1553, 2010.

[7] G. Li, N. Xi, H. Chen, C. Pomeroy and M. Prokos, ""Videolized" atomic force microscopy for interactive nanomanipulation and nanoassembly," IEEE Trans. Nanotechnol., vol. 4, no. 5, pp. 605–615, 2005.

[8] M. Sitti and H. Hashimoto, "Controlled Pushing of Nanoparticles: Modeling and Experiments," IEEE/ASME Trans. on Mechatronics, vol. 5, no. 2, 2000.

[9] Q. Yang and S. Jagannathan, "Atomic force microscope-based nano manipulation with drift compensation," International Journal of Nanotechnology, vol. 3, no.4, pp. 527-544, 2006.

[10] C.D. Onal, O. Ozcan, M. Sitti, "Automated 2-D Nanoparticle Manipulation Using Atomic Force Microscopy," IEEE Transactions on Nanotechnology, vol.10, no.3, pp.472-481, 2011

[11] J.C. Hsu, H.L. Lee and W.J. Chang, "Flexural Vibration Frequency of Atomic Force Microscope Cantilevers using the Timoshenko Beam Model," Nanotechnology, vol. 18, no. 28, pp. 285503, 2007

[12] S. Eslami andN. Jalili, "Adaptive trajectory control of microcantilever's tip utilised in atomic force microscopy-based manipulation," International Journal of Control, vol. 84, no. 12, pp. 1945-1955, 2011

[13] H. K. Khalil, Nonlinear Systems, 3rd ed. Upper Saddle River, NJ: Prentice-Hall, 2002.

[14] M. Krstic, I. Kanellakopoulos, P. Kokotovicet al., Nonlinear and adaptive control design, Wiley: New York, 1995.

[15] O.M. El Rifai and K. Youcef-Toumi, "On automating atomic force microscopes: an adaptive control approach," Control Engineering Practice, vol. 15, no. 3,pp. 349–361. 2007.

[16] C. Cao and N. Hovakimyan, "Guaranteed transient performance with L1 adaptive controller for systems with unknown time-varying parameters and bounded disturbances: Part I," Proc. of American Control Conference, pp. 3925-3930, 2007

[17] Q.Yang, S. Jagannathan and E. W. Bohannan, "Automatic drift compensation using phase-correlation method for nanomanipulation," IEEE Transaction on Nanotechnology, vol. 7, no.2, pp. 209-216, 2008.

[18] L.Liu, N. Xi, Y.Wang, Z. Dong, "Drift Compensation and Faulty Display Correction in Robotic Nano Manipulation," Journal of Nanoscience and Nanotechnology. vol. 10, no. 11, pp.7010-7014, 2010.

[19] J. Lü, M. Ye, N. Duan andB. Li, "Enzymatic digestion of single DNAmolecules anchored on nanogold-modified surfaces," Nanoscale Research Letters, vol. 4, no. 9, pp. 1029-1034, 2009.

[20] T. R. Hicks and P. D. Atherton, The Nano Positioning Book, Bracknell,U.K.: Queensgate Inst., 1997.